SCIENCE CHINA
Information Sciences

• RESEARCH PAPERS •

November 2010 Vol. 53 No. 11: 2363–2376
doi: 10.1007/s11432-010-4093-7

Accurate location of all surface wave modes for Green's functions of a layered medium by consecutive perturbations

SONG Zhe*, ZHOU HouXing*, HU Jun, LI WeiDong & HONG Wei

State Key Laboratory of Millimeter Waves, School of Information Science and Engineering, Southeast University, Nanjing 210096*, China*

Received March 26, 2010; accepted June 30, 2010

Abstract In this paper, an efficient method is proposed to quickly and accurately locate all the surface wave modes of spectral Green's functions of a layered medium. This method consists of two parts. In the first part, all the surface wave poles without considering the medium loss are located by a modified dichotomy on the real axis in the complex plane. In the second part, consecutive perturbations with respect to the medium loss are performed, which means that the medium loss is increased step by step from zero to the given value, and at each step, the Newton-Raphson algorithm is employed to find all the current poles, with the poles at the previous step as initial values. The residues of the surface wave poles are analytically calculated without any contour integral. The whole procedure is based on the recursively rational forms of spectral Green's functions. As an application, all the surface wave poles and their residues obtained by the method proposed in this paper are applied in evaluation of the spatial Green's functions by the discrete complex image method. Some numerical examples are provided to validate the correctness and efficiency of the proposed method.

Keywords Green's function, Sommerfeld integral, surface wave pole, perturbation, discrete complex image method

Citation Song Z, Zhou H X, Hu J, et al. Accurate location of all surface wave modes for Green's functions of a layered medium by consecutive perturbations. Sci China Inf Sci, 2010, 53: 2363–2376, doi: 10.1007/s11432-010-4093-7

1 Introduction

With the development of microwave monolithic integrated circuits (MMIC) and the great progress in low temperature co-fired ceramics (LTCC) techniques, the numerical modeling and simulation of circuits in a planar layered medium structure have received intense attention in the microwave community [1–4]. The method of moments (MoM) [5] based on the mixed-potential integral equation (MPIE) [6–8] is one of the full wave methods most suitable for the rigorous analysis of circuits in a layered medium structure. The spatial Green's functions constitute an important foundation of the MPIE, and then how to efficiently calculate the Green's functions becomes an important topic. Based on the geometry characteristics of a layered medium structure, the spectral Green's functions can be easily derived and expressed in finite recursive forms [9, 10], and then their counterparts in the spatial domain can be formally expressed in

*Corresponding authors (email: zhesong@emfield.org, hxzhou@emfield.org)

terms of the well-known Sommerfeld integrals (SI), whose integral kernels are Bessel or Hankel functions [11]. For the fast and accurate calculation of SI, several kinds of methods have been proposed and studied [12], including the steepest descent path (SDP) [2, 11, 13, 14], the discrete complex image method (DCIM) [15, 16], and its two-level version [17], the generalized pencil of function method (GPOF) [18], the vector fitting method [19–21], the contraction mapping method [22], the fast all modes (FAM) method combined with the numerical modified steepest path (NMSP) [23–25], and so on.

In the original DCIM [15], surface wave poles (SWP) should be extracted, which could facilitate the function fitting either by the Prony or GPOF methods. Also, in SDP, the contributions of both surface and leaky wave poles (LWP) involved need to be included. Therefore, how to locate the poles effectively has historically attracted great attention [26–30]. In this paper, only SWP is considered.

A quartation based on contour integrals was proposed for searching for the SWPs in an interested region on the top Riemann sheet [31, 32] in 2000. This method was easy to comprehend and realize. Experiments show that there exist a trade-off between the accuracy of the root and that of the adaptive integration. Moreover, the integration paths may become extremely adjacent to some genuine poles which makes the integration very time-consuming.

The vector fitting scheme was suggested for the spatial Green's functions [20]. Based on the explanation on the physical behavior of waves in a layered medium, the spatial Green's function is directly approximated by a finite sum of some spherical and cylindrical waves, where all the SWPs should be found through matrix iterations [33]. This method may cause redundancies since it has to assume enough poles on the real axis for the lossless case and then do iterations. Actually, this scheme essentially suffers from almost the same difficulty as the SWP-locating in the DCIM.

For the lossless-medium case, it was suggested that the Newton-Raphson algorithm be adopted to find out all the SWPs on the real axis [27, 34, 35] and then the contour integrals were employed to evaluate the residues of these poles. This scheme cannot be directly extended to the lossy-medium case since no available root-searching paths have been found yet. The argument principle [36] method was also introduced to do zero-searching for planar layered waveguides [30, 37, 38]. It can be seen from the details of [38] that the term "pole-free" should be "branch-free" in the present problem. If the reciprocal form was taken to do zero-searching, as with [38], then it could encounter pole points corresponding to zero points, as shown in section 5 of this paper.

The characteristic equation of a microstrip structure can be analytically derived, which is quite convenient for theoretical analyses. Recently, the fast all modes (FAM) method combined with the numerical modified steepest path (NMSP) has been proposed for evaluating the spatial Green's functions of a microstrip structure [23, 24]. In this method, both the SWPs on the top Riemann sheet and the leaky wave poles (LWPs) on the bottom Riemann sheet are located and extracted. This method has higher accuracy even if the substrate has a moderate thickness. This method has been further developed since as locating all modes based on the local Taylor expansion was established [39]. Just recently, one type of extension of FAM/NMSP to multilayer structures and lossy cases [25] has been proposed, which locates both the SWPs and LWPs by the Newton-Raphson refinement with those poles under the lossless case as initial values. This method expresses the generalized reflection coefficients in a determinant form, through which all the modes can be found by solving a polynomial equation when the sine and cosine functions are approximated by Taylor expansions. There could be some uncertainty on the determinant when the number of layers becomes larger, since the dimension of matrix is more than two times larger of that.

Besides these, schemes for avoiding the extraction of SWP also have been considered by researchers. Recently, two such schemes have been proposed for the lossless-medium case. One suggested to make the sampling path in the fitting process as close to the pole locations as possible in order to get sufficient information about the singularities [40]. The other employed the modified matrix pencil method to do complex exponential fitting [41, 42]. Either of the two schemes can improve the DCIM to a certain extent. But they still face the convergence problem in the far field region which is mainly influenced by surface wave modes for the lossless-medium case.

In this paper, an efficient method is proposed to quickly and accurately locate all the SWPs of spectral

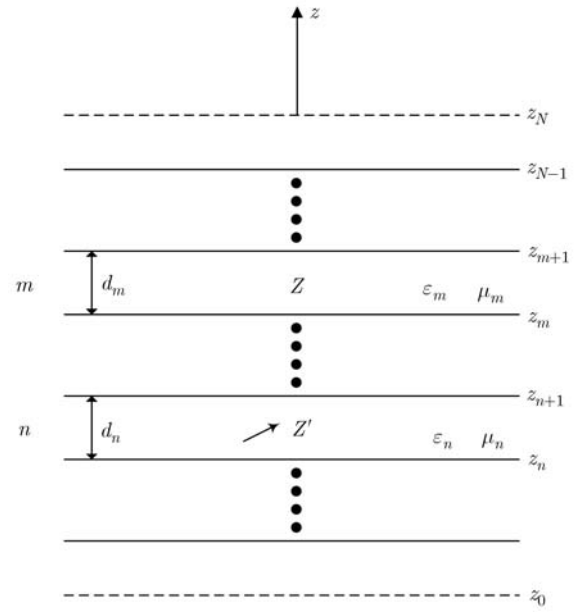

Figure 1 A layered medium structure.

Green's functions of a layered medium. This method consists of two parts. In the first part, all the SWPs, without considering the medium loss, are located by a dichotomy on the real axis. In the second part, consecutive perturbations with respect to the medium loss are performed, which means that the medium loss is increased step by step from zero to the given value, and at each step, the Newton-Raphson algorithm is employed to update all the poles. The residues of SWPs are analytically calculated without any contour integrals. As an application, all the SWPs and their residues obtained by the method proposed in this paper are applied in the evaluation of spatial Green's functions by DCIM. The model considered in this paper is shown in Figure 1 and the notations in [7] are adopted. The time factor is implied in this paper.

2 Rational forms of spectral Green's functions

The structure depicted in Figure 1 is assumed to be laterally infinite. Layer i is characterized by relative permittivity $\varepsilon_{r,i}$ and relative permeability $\mu_{r,i}$. The thickness of ith layer is $d_i = z_{i+1} - z_i$. The top and the bottom layers may be either dielectric or PEC. Assume the source point and the field points are in layer n and layer m, respectively.

Based on the equivalent transmission line network [43], all the spectral Green's functions can be expressed in terms of the transmission line Green's functions (TLGF) as follows [7]:

$$\widetilde{G}^A_{xx} = \frac{1}{j\omega\mu_0} V_i^h, \tag{1}$$

$$\frac{j}{k_x}\widetilde{G}^A_{xz} = \frac{j}{k_y}\widetilde{G}^A_{yz} = \frac{\mu_{r,n}}{k_\rho^2}(V_v^h - V_v^e), \tag{2}$$

$$\frac{j}{k_x}\widetilde{G}^A_{zx} = \frac{j}{k_y}\widetilde{G}^A_{zy} = \frac{\mu_{r,n}}{k_\rho^2}(I_i^h - I_i^e), \tag{3}$$

$$\widetilde{G}^A_{zz} = \frac{1}{j\omega\varepsilon_0}\left[\left(\frac{\mu_{r,m}}{\varepsilon_{r,n}} - \frac{\mu_{r,n}}{\varepsilon_{r,m}}\frac{k_{z,m}^2}{k_\rho^2}\right) I_v^e + \frac{k_0^2\mu_{r,m}\mu_{r,n}}{k_\rho^2} I_v^h\right], \tag{4}$$

$$\widetilde{G}^\Phi = \frac{j\omega\varepsilon_0}{k_\rho^2}(V_i^e - V_i^h). \tag{5}$$

The TLGFs can be further expressed in terms of the so-called generalized reflection coefficients [2, 7]. Formulae (62), (66) and (67) in [7] are very compact, but it is not easy to search their poles. Evidently it

is inconvenient to directly change these forms into explicit rational forms of all $k_{z,n}$ since the generalized reflection coefficients are recursive. However, the acquirement of their implicit rational forms is indeed feasible. For clarity, a proper notation is introduced. If A is a rational form of all $k_{z,n}$, then A may be written as

$$A = \frac{A^{>}(\text{numerator})}{A^{<}(\text{denominator})}, \tag{6}$$

where $A^{>}$ and $A^{<}$ are both polynomial forms of all $k_{z,n}$, and are called the numerator and the denominator of A, respectively. Based on this stipulation, each formula from (59) to (61) in [7] can be rewritten as a rational form of all $k_{z,n}$ whose numerator and denominator can be calculated recursively. The details about the derivation are shown in Appendix. Therefore, the spectral Green's functions can be easily rewritten as

$$\widetilde{G}^{A}_{xx} = \frac{1}{j\omega\mu_0}\frac{V_i^{h,>}}{V_i^{h,<}}, \tag{7}$$

$$\frac{j}{k_x}\widetilde{G}^{A}_{xz} = \frac{j}{k_y}\widetilde{G}^{A}_{yz} = \frac{\mu_{r,n}(V_v^{h,>}\cdot V_v^{e,<} - V_v^{e,>}\cdot V_v^{h,<})}{k_\rho^2\cdot V_v^{h,<}\cdot V_v^{e,<}}, \tag{8}$$

$$\frac{j}{k_x}\widetilde{G}^{A}_{zx} = \frac{j}{k_y}\widetilde{G}^{A}_{zy} = \frac{\mu_{r,n}(I_i^{h,>}\cdot I_i^{e,<} - I_i^{e,>}\cdot I_i^{h,<})}{k_\rho^2\cdot I_i^{h,<}\cdot I_i^{e,<}}, \tag{9}$$

$$\widetilde{G}^{A}_{zz} = \frac{1}{j\omega\varepsilon_0}\frac{\left[\begin{array}{l}\left(\mu_{r,m}\varepsilon_{r,m}k_\rho^2 - \mu_{r,n}\varepsilon_{r,n}k_{z,m}^2\right)\cdot I_v^{e,>}\cdot I_v^{h,<}\\ +k_0^2\mu_{r,m}\mu_{r,n}\varepsilon_{r,n}\varepsilon_{r,m}\cdot I_v^{e,<}\cdot I_v^{h,>}\end{array}\right]}{\varepsilon_{r,n}\varepsilon_{r,m}k_\rho^2\cdot I_v^{e,<}\cdot I_v^{h,<}}, \tag{10}$$

$$\widetilde{G}^{\Phi} = \frac{j\omega\varepsilon_0(V_i^{e,>}\cdot V_i^{h,<} - V_i^{h,>}\cdot V_i^{e,<})}{k_\rho^2\cdot V_i^{e,<}\cdot V_i^{h,<}}. \tag{11}$$

To analytically calculate the residues of all the SWPs, the derivatives of the denominators of the spectral Green's functions with respect to k_ρ are also needed, and the corresponding expressions are also shown in Appendix.

3 Location of SWP for lossless-medium case by dichotomy

As is well known [4], for the lossless-medium case, all the SWPs of a spectral Green's function are located inside a finite interval on the real axis, while they should be zero points of first order of the denominator for physical reasons. Hence, the dichotomy on this interval might find out all the SWPs. However, the ordinary dichotomy would lose some SWPs because of an insufficient initial division. Certainly, experience can help one to select a proper initial division, but such a strategy is uncontrollable in applications. In this paper, we provide an analysis for selecting the initial division and construct a modified dichotomy for finding all SWPs for the lossless-medium case.

For the lossless case, according to the characteristic of the denominator of the spectral Green's functions, the SWPs exist between two adjacent crest and trough points. Therefore, the initial division is closely related to the minimum distance between two adjacent crest and trough points of the denominators. It is easily understood that the denominator of the spectral Green's functions exhibit higher oscillation if the thickness of the structure is large. Hence, the multilayer structure is artificially degenerated to a simple microstrip model, where the total thickness is h, and $\varepsilon_{\max}$ and $\mu_{\max}$ are used, as shown in Figure 2. By using the formulae given in [44], the Green's functions of the microstrip structure can be derived in explicit form. Taking the denominator $\widetilde{G}_{xx}^{A,<}$ of $\widetilde{G}_{xx}^{A}$ as an example, we have

$$\widetilde{G}_{xx}^{A,<} = k_{\max,z}\cos(k_{\max,z}h) + jk_{0,z}\sin(k_{\max,z}h). \tag{12}$$

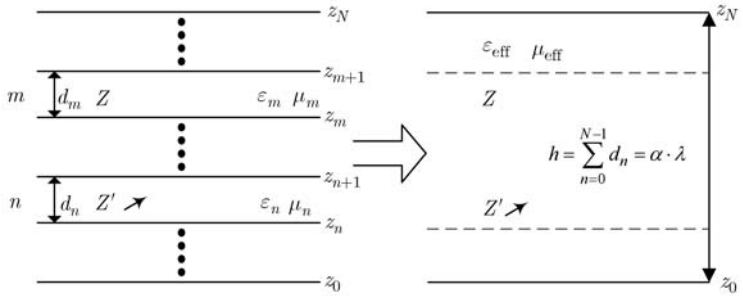

Figure 2 Degeneration from a multilayered to a microstrip structure.

Referring to [39], the characteristic equation of $\widetilde{G}_{xx}^{A,<}$ can be transformed to

$$\begin{cases} I = \cos(2k_{\max,z}h) + \left(\dfrac{2(k_{\max,z}h)^2}{r^2} - 1\right), \\ r^2 = k_{\max}^2 - k_0^2. \end{cases} \tag{13}$$

Clearly, $I(k_\rho)$ exhibits an oscillatory characteristic due to $\cos(2k_{\max,z}h)$. To estimate the minimum distance between two adjacent crest and trough point $T_{\min}$, only $\cos(2k_{\max,z}h)$ are taken into account, and we have

1) If $\alpha < \dfrac{1}{4\sqrt{\min\limits_{1\leqslant i\leqslant N-1}\{\varepsilon_{r,i}\mu_{r,i}\}-1}}$, the number for the initial division may be selected as 5. This is sufficient for isolating SWP.

2) If $\alpha >= \dfrac{1}{4\sqrt{\min\limits_{1\leqslant i\leqslant N-1}\{\varepsilon_{r,i}\mu_{r,i}\}-1}}$, the minimum distance between two adjacent crest and trough points is a function of the index m:

$$T(m) = k_\rho(m) - k_\rho(m+1) = \left(\sqrt{\varepsilon_{\max}\mu_{\max} - \left(\frac{m}{4\alpha}\right)^2} - \sqrt{\varepsilon_{\max}\mu_{\max} - \left(\frac{m+1}{4\alpha}\right)^2}\right) \cdot k_0. \tag{14}$$

This $T(m)$ is monotonically increasing, which indicates that the minimum value of $T(m)$ is reached at $m = 1$. Therefore,

$$T_{\min} \approx k_\rho(1) - k_\rho(2). \tag{15}$$

To accelerate the whole dichotomy procedure, a factor L may be needed to modify the number of initial division. Finally, we have,

$$N = (\text{Int}[(k_{\max} - k_0)/T_{\min}] + 1) \times L, \tag{16}$$

where Int represents the round function towards minus infinity.

Owing to the high nonlinearity of the characteristic function, either the crest or trough points maybe almost tangent to the real axis. This could enhance the computation load if we just simply increase the initial division for dichotomy. Therefore, a modified dichotomy is designed and applied, which is based on analytical derivatives of the functions. The details can be explained as follows.

Let (x_1, x_2) be a starting subinterval of $(k_0, k_{\max})$, as let $f(x_1)(f(x_2))$ and $f'(x_1)(f'(x_2))$ be the function value and the derivative value at the ends, respectively. By properly selecting on the value of N, we have the following three cases:

Case I: If

$$\begin{cases} f(x_1) \cdot f(x_2) \geqslant 0, \\ f'(x_1) \cdot f'(x_2) \geqslant 0, \end{cases} \tag{17}$$

there exists no zero point inside (x_1, x_2).

Case II: If

$$f(x_1) \cdot f(x_2) \leqslant 0, \tag{18}$$

there exists one and only one zero point inside (x_1, x_2).

Case III: If

$$\begin{cases} f(x_1) \cdot f(x_2) \geqslant 0, \\ f'(x_1) \cdot f'(x_2) \leqslant 0, \end{cases} \tag{19}$$

either no zero point or two zero points exist inside (x_1, x_2), depending upon the value of $f(x)$ at the crest or trough points within (x_1, x_2). In this situation, the ordinary dichotomy is first used to search for the zero point x_3 of $f'(x)$ within (x_1, x_2). Then, the interval is divided into two subintervals (x_1, x_3) and (x_3, x_2). It is easily known that it is monotonic in both the two subintervals. Hence, we can go back to Case I or Case II. Some important points are stated as follows.

1) In the dichotomy process, the TE and TM modes of TLGFs are treated individually, and for each mode, only those points where the amplitudes vanish rapidly are zero points of the denominators.

2) Not all of the zero points of the denominator are SWPs. That is because after the rational forms are applied recursively, the operation of reduction will introduce some false poles, which are zero points of the numerators simultaneously. A simple way to filter out these removable singular points is to calculate their residues, which have very small absolute values.

3) The dichotomy process is not capable of searching for the zero points of higher order of a function. Fortunately, the poles of the spectral Green's function are all the zero points of first order of the denominator for physical reasons.

4 Location of SWP for lossy-medium case by consecutive perturbations

Several papers have applied and verified the efficiency of Newton-Raphson refinement when we want to get SWPs for the lossy-medium case by using those in the lossless case as initial values [24, 25, 34]. In this paper, the Newton-Raphson algorithm is employed more directly because we obtained the analytical denominator of spectral Green's functions, which implies that the derivatives of these functions can also be simultaneously analytically derived.

However, since the Newton-Raphson algorithm is very sensitive to the selection of initial values [46], the changes in the coefficients of functions should be slight. In our problem, if some perturbations of the medium parameters occur, the former zero points should be very close to the current ones as long as the perturbations are sufficiently slight, which could ensure the success of Newton iterations. From this point of view, we can establish an algorithm procedure with two parts.

Part 1: All the SWPs without considering the medium loss are found by the dichotomy presented in section 3.

Part 2: Consecutive perturbations with respect to the medium loss are performed. That is, the medium loss is increased step by step to ensure the success of the Newton-Raphson iterations.

It is worth emphasizing that, under a large perturbation, the Newton-Raphson algorithm could not converge to the genuine root or even failed to converge [46]. A larger perturbation would cause the algorithm to depart from the correct tracking path and go to an adjacent one, as shown in Figure 3. In this sketch, the root-tracking paths are depicted by dashed lines, where A_i, B_i and C_i stand for different roots at the ith perturbation step. For the slight-perturbation case, like at steps 1 and 2, all the roots can be correctly found by the Newton-Raphson algorithm. Whereas, for the large perturbation case, like step 3, the iteration departs from the C-path and mistakenly reaches B_3. This results in losing a genuine root C_3. An appropriate remedy is to append one or more steps between steps 2 and 3, as shown in Figure 3. Considering the fact that perturbations on the imaginary parts of the medium parameters do not change the number of the SWPs, we would rather implement Part 2 by means of a feedback system that is illustrated by a diagram as shown in Figure 4.

Actually, there exists a trade-off between the number of perturbation steps and the cost of the Newton-Raphson iterations. The loss tangent of a medium is presented as a negative imaginary part because of the time factor. Based on plenty of experiments, a menu of empirical values for the perturbation steps are shown in Table 1, and can be selected as an initial M for the feedback system. For the multilayered

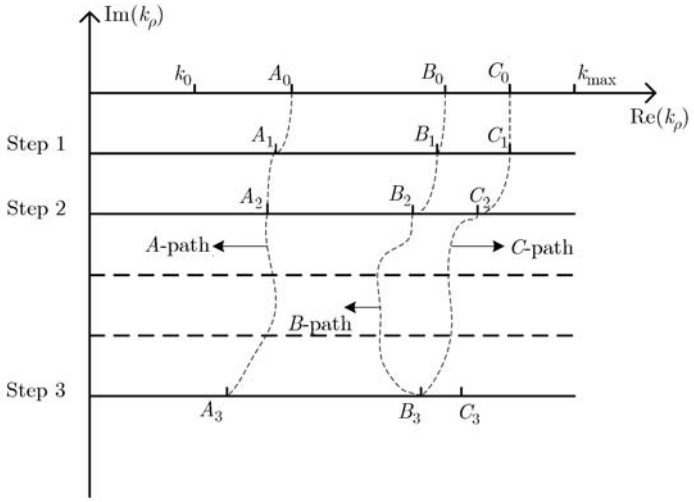

Figure 3 Root-searching paths for the large-perturbation case.

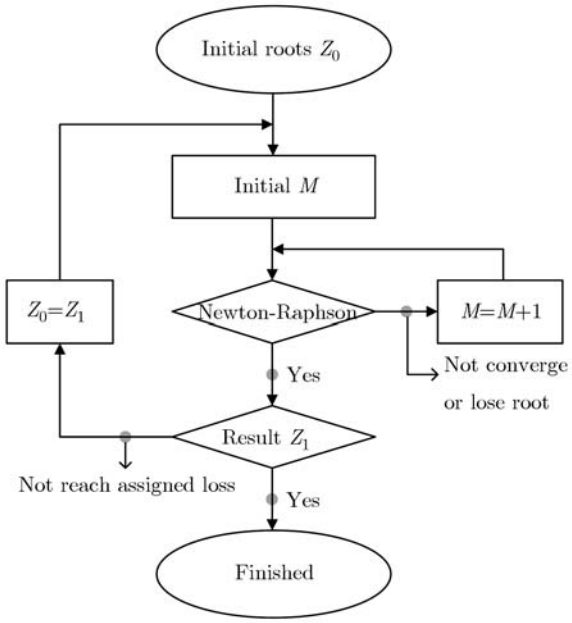

Figure 4 Feedback system for the consecutive perturbation method.

Table 1 Reference number of perturbations for lossy-medium case

Initial M	ε''
1	$\varepsilon'' < 0.004$
2	$\varepsilon'' < 0.04$
4	$\varepsilon'' < 0.4$
10	$\varepsilon'' < 2$
20	$\varepsilon'' < 4$
30	$\varepsilon'' < 8$
40	$\varepsilon'' <= 10$

medium, we take ε'' as $\max_{1\leqslant i\leqslant N-1}\{\varepsilon_i''\}$ to select M and take $\Delta\varepsilon_i'' = \varepsilon_i''/M(\forall i)$ as the increment of ith layer medium at each perturbation step 1.

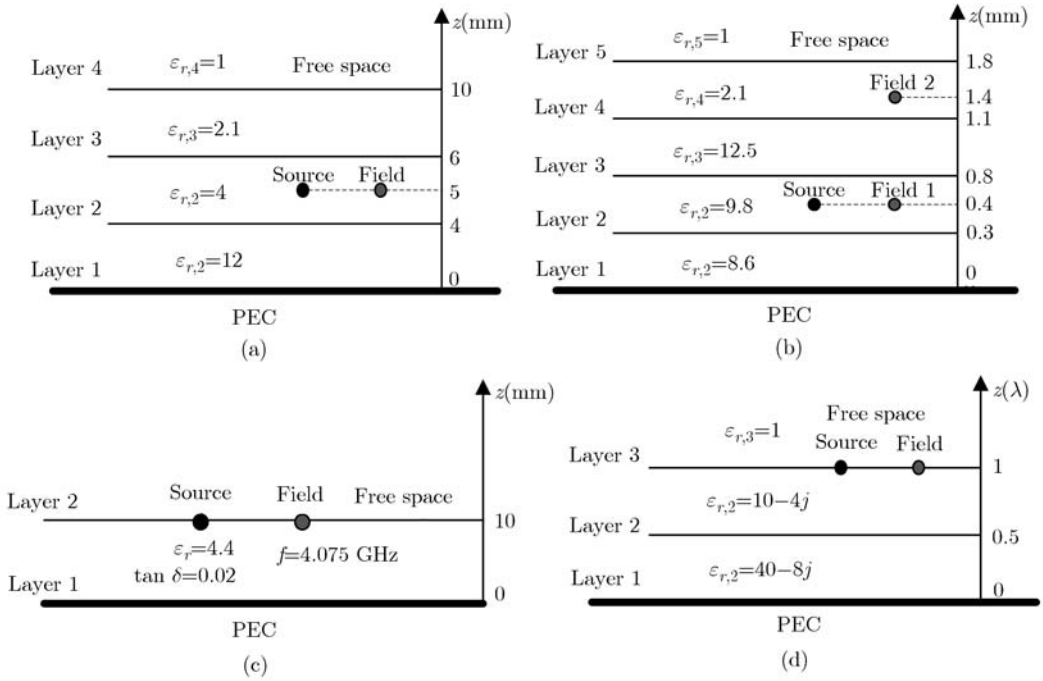

Figure 5 Modeling for numerical examples. (a) Example A; (b) example B; (c) example C; (d) example D.

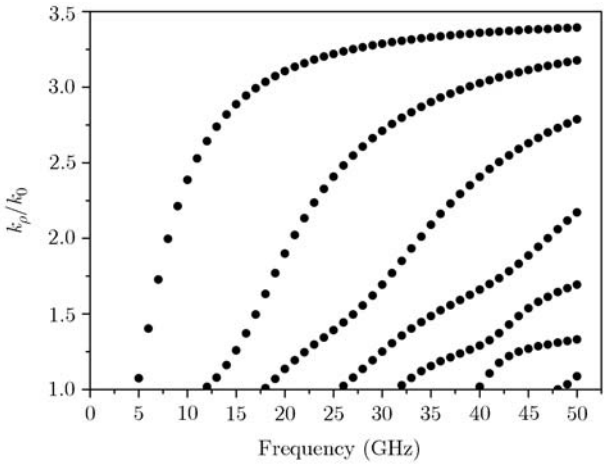

Figure 6 Surface wave poles of Case A.

5 Numerical results and discussion

In this section, four numerical examples are provided to validate the method proposed in this paper (see Figure 5). The application of the SWPs and their residues into DCIM is also realized for both the lossless and lossy cases. All the programming code was written in C language and ran on a P4-2.5 GHz with 3.25 GB RAM. For validation and comparison, the quartation method was also realized. The time cost (comparing to the quartation method) of the proposed method is satisfactory and superior.

• Example A: Accurate location of the SWPs for lossless case. All SWPs of this structure at different frequencies are located with an accuracy of 10^{-10} and shown in Figure 6. The results have been proved by means of the quartation method. The average time cost of the dichotomy for each frequency point is around 75 ms, while that of quartation method is around 1100 ms and is proportional to the number of poles.

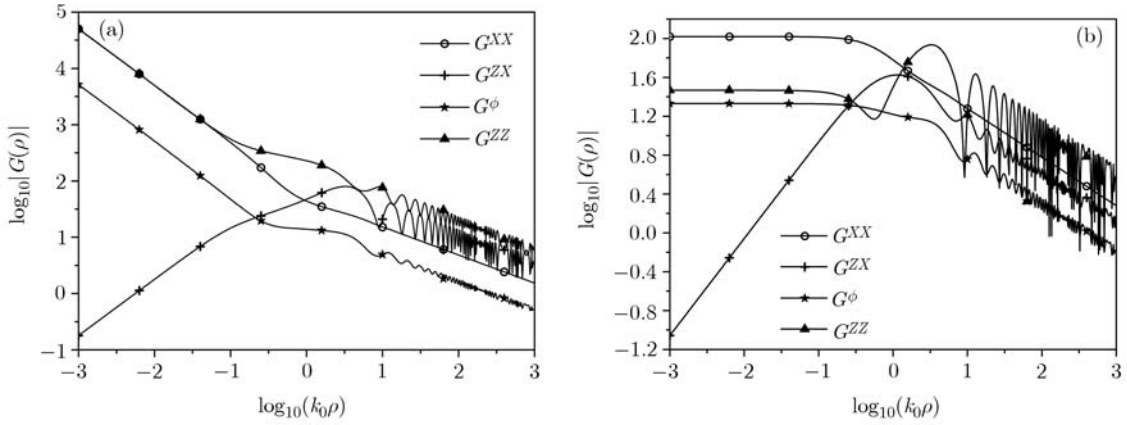

Figure 7 Spatial Green's functions of the model for Case B. (a) Field point 1; (b) field point 2.

Table 2 Surface wave poles and residues

Function	SWPs (k_0)	abs (Residues)	Time cost (s)
$\widetilde{G}_{xx}^{A,<}$	1.7365	0.1465	0.015
$\widetilde{G}_{zx}^{A,<}$	1.7365, 2.4354	0.0003, 0.0001	0.072
$\widetilde{G}_{zz}^{A,<}$	1.7365, 2.4354	0.5749, 0.1244	0.100
$\widetilde{G}_{\Phi}^{A,<}$	1.7365, 2.4354	0.0486, 0.0046	0.042
$\widetilde{G}_{xx}^{A,<}$	1.6933	0.1845	0.233
$\widetilde{G}_{zx}^{A,<}$	1.7385, 2.4327	0.0001, 0.00001	0.356
$\widetilde{G}_{zz}^{A,<}$	1.7365, 2.4354	0.2513, 0.1827	0.415
$\widetilde{G}_{\Phi}^{A,<}$	1.7365, 2.4354	0.0600, 0.0085	0.394

• Example B: Classical 4-layer model. This model has been analyzed by several papers, e.g. [31, 34, 40]. The operating frequency is 30 GHz. In this model, the numerators of V_i^e also contain zero points at $1.7907k_0$ and $2.9787k_0$, while V_i^h contain zero point at $1.0041k_0$, which implies that taking the reciprocal form of the TLGFs will introduce pole-singularities at the same time. All the surface wave poles and their residues are listed in Table 2, and the spatial Green's functions are shown in Figure 7.

• Example C: When the SWP is very close to the branch point. This model has been analyzed by [47–49]. The SWPs associated with the TE and TM modes for the lossless case are $1.000014397k_0$ and $1.478658455k_0$, respectively, while those for the lossy case are $(0.999315104 - 0.000214412i)k_0$ and $(1.478562900 - 0.018132860i)k_0$, respectively. The SWPs also have been validated by the quartation method. The spatial Green's function of G^{Φ} are calculated and validated by DCIM and SI, respectively, and are shown in Figure 8. From Figure 8(a), good agreement has been found between DCIM and SI. However, the DCIM no longer works well for the lossy case especially in far field region, shown in Figure 8(b). This phenomenon could be well explained by the theory described in [47, 49, 50] that reveals that the contribution of the continuous spectrum should be included in both the lossless and lossy medium cases, and the Green's functions in the far field region are mainly affected by the continuous spectrum for the lossy medium case. In this situation, the FAM/NMSP method [25] or the method used in [39] could be adopted.

• Example D: Dense distribution of SWPs for the lossy case. This model is designed to have up to 7 TE modes and 7 TM modes. With the increase of the number of surface wave modes, some TE and TM modes could be very close to each other, so called coupling modes, as shown in Figure 9. Fortunately, since the modified dichotomy method treats TE or TM modes individually, we can still separate them with very high accuracy. The final results have been validated by the quartation method, as is shown in Table 3, while the total time cost of the dichotomy and the Newton-Raphson iteration is 0.2630 s.

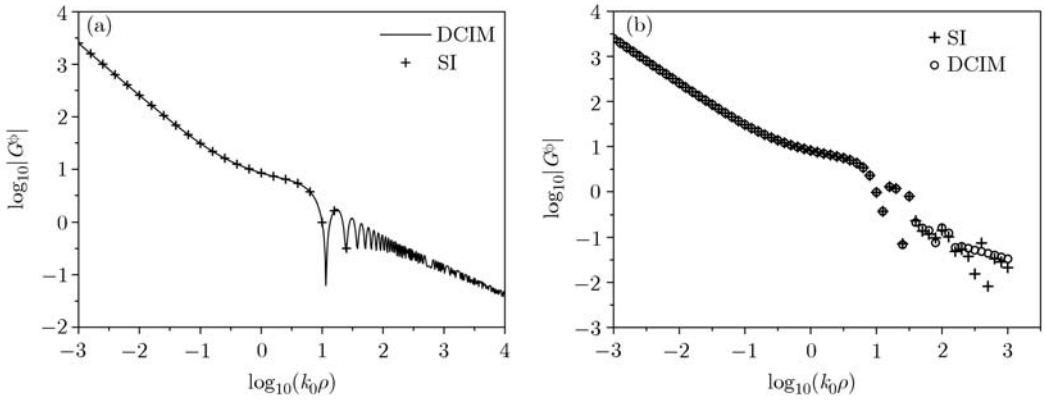

Figure 8 Spatial Green's function for the model of Case C. (a) Lossless case; (b) lossy case.

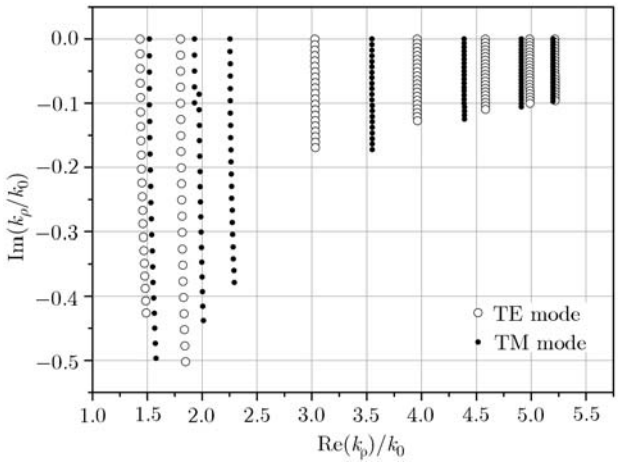

Figure 9 Roots tracking process in heavy lossy Case D.

Table 3 TE and TM surface wave modes of Case D

TE modes (k_0)	TM modes (k_0)
1.4895–0.4259i	1.5784–0.4968i
1.8482–0.5022i	2.0107–0.4381i
3.0318–0.1691i	2.2921–0.3784i
3.9617–0.1273i	3.5515–0.1721i
4.5824–0.1095i	4.3896–0.1247i
4.9871–0.1004i	4.9102–0.1056i
5.2174–0.0959i	5.1993–0.0970i

6 Conclusions

In this paper, a consecutive perturbation method is proposed to fast and accurately locate all SWPs for spectral Green's functions of layered medium. The fractional forms of TLGFs are derived, based on which all the SWPs for lossless-medium case can be found by the dichotomy with very high accuracy. Sequentially, the medium loss are increased step by step from zero to any given value, and at each perturbation step, the Newton-Raphson algorithm is employed to find out all current poles with the poles at the previous step as initial values. The residues of the surface wave poles are analytically calculated without any contour integrals. With the surface wave poles and their residues obtained by the proposed method, they were applied in the evaluation of spatial Green's functions by the one-level DCIM. The numerical examples can validate the correctness and efficiency of this method. In the near future, this method will be applied in locating the LWPs for accurate evaluation of spatial Green's functions.

Acknowledgements

This work was supported by the National Basic Research Program of China (Grant Nos. 2009CB320203, 2010CB327400), the Science Fund for Creative Research Groups of China (Grant No. 60921063), the National Science Fund for Young Scholars of China (Grant No. 60901013), and the National Nonprofit Industry Specific Research Program of China (Grant No. 201110046-2).

References

1 Mosig J R. Numerical Techniques for Microwave and Millimeter-Wave Passive Structures. Itoh T, ed. New York: Wiley, 1989, ch. 3
2 Chew W C. Waves and Fields in Inhomogeneous Media. ser. Electromagn Waves. Piscataway, NJ: IEEE Press, 1995
3 Chew W C, Jin J M, Michielssen E, et al. Efficient Algorithm in Computational Electromagnetics. Boston, London: Artech House, 2001
4 Fang D G. Antenna Theory and Microstrip Antennas. Beijing: Science Press, 2006
5 Harrington R F. Field Computation by Moment Methods. Melbourne, FL: Krieger, 1983
6 Michalski K A, Zheng D. Electromagnetic scattering and radiation by surfaces of arbitrary shape in layered media, Part I: Theory. IEEE Trans Anten Propag, 1990, 38: 335–344
7 Michalsky K A, Mosig J R. Multilayered media Green's functions in integral equation formulations. IEEE Trans Micro Theory Tech, 1997, 45: 508–519
8 Bernal J, Medina F, Boix R R, et al. Fast full-wave analysis of multistrip transmission lines based on MPIE and complex image theory. IEEE Trans Microw Theory Tech, 2000, 48: 445-452
9 Aksun M I, Mittra R. Derivation of closed-form Green's functions for a general microstrip geometry. IEEE Trans Microw Theory Tech, 1992, 40: 2055–2062
10 Dural G, Aksun M I. Closed-form Green's functions for general sources and stratified media. IEEE Trans Microw Theory Tech, 1995, 43: 1545-1551
11 Collin R E. Field Theory of Guided Waves. New York: McGraw-Hill, 1960
12 Aksun M I, Dural G. Clarification of issues on the closed-form Green's functions in stratified media. IEEE Trans Anten Propag, 2005, 53: 3644–3653
13 King R W P. The electromagnetic field of a horizontal electric dipole in the presence of a three-layered region. J Appl Phys, 1991, 69: 7985–7995
14 Cui T J, Chew W C. Fast evaluation of Sommerfeld integrals for EM scattering and radiation by three dimension buried objects. IEEE Trans Geosci Remote Sens, 1999, 37: 887–900
15 Fang D G, Yang J J, Delisle G Y. Discrete image theory for horizontal electric dipoles in a multilayered medium. IEE Proc H, 1988, 135: 297–303
16 Kipp R A, Chan C H. Complex image method for sources in bounded regions of multilayer structures. IEEE Trans Microw Theory Tech, 1994, 42: 860–865
17 Aksun M I. A robust approach for the derivation of closed form Green's functions. IEEE Trans Microw Theory Tech, 1996, 44: 651–658
18 Hua Y, Sakar T K. Generalized pencil-of-function method for extracting poles of an EM system from its transient response. IEEE Trans Anten Propagat, 1995, 37: 229–234
19 Gustavsen B, Semlyen A. Rational approximation of frequency domain responses by vector fitting. IEEE Trans Power Delivery, 1999, 14: 1052–1061
20 Kourkoulos V N, Cangellaris A C. Accurate approximation of Greens functions in planar stratified media in terms of a finite sum of spherical and cylindrical waves. IEEE Trans Anten Propag, 2006, 54: 1568–1576
21 Polimeridis A G, Yioultsis T V, Tsiboukis T D. A robust method for the computation of Green's functions in stratified media. IEEE Trans Anten Propag, 2007, 55: 1963–1969
22 Teo S A, Leong M S, Chew S T, et al. Complete location of poles for thick lossy grounded dielectric slab. IEEE Trans Microw Theory Tech, 2002, 50: 440–445
23 Tsang L, Wu B. Electromagnetic fields of Hertzian dipoles in layered media of moderate thickness including the effects of all modes. IEEE Anten Wirel Propag Lett, 2007, 6: 316–319
24 Wu B, Tsang L, Ong C J. Fast all modes (FAM) method combined with NMSP for evaluating spatial domain layered medium Green's functions of moderate thickness. Microw Opt Tech Lett, 2007, 49: 3112–3118
25 Wu B, Tsang L. Fast computation of layered medium of Green's functions of multilayers and lossy media using fast all-modes method and numerical modified steepest descent path method. IEEE Trans Microw Theory Tech, 2008, 56: 1446–1454
26 Marin M A, Barkeshli S, Pathak P H. On the location of proper and improper surface wave poles for the grounded

dielectric slab. IEEE Trans Anten Propag, 1990, 38: 570–573
27 Liu Y, Li L W, Yeo T S, et al. Application of DCIM to MPIE-MoM analysis of 3-D PEC objects in multilayered media. IEEE Trans Anten Propag, 2002, 50: 157–162
28 Neve M J, Paknys R. A technique for approximating the location of surface- and leaky-wave poles for a lossy dielectric slab. IEEE Trans Anten Propag, 2006, 54: 115–120
29 Simsek E, Liu Q H, Wei B. Singularity subtraction for evaluation of Green's function for multilayer media. IEEE Trans Microw Theory Tech, 2006, 54: 216–225
30 Mesa F, Horno M. Computation of proper and improper modes in multilayered bianisotropic waveguides. IEEE Trans Microw Theory Tech, 1995, 43: 233–235
31 Ling F. Fast electromagnetic modeling of multilayer microstrip antennas and circuits. Ph. D. Thesis in Elect. Eng. Urbana-Champaign: Illinois Univ., 2000
32 Ling F, Jin J M. Discrete complex image method for Greens functions of general multilayer media. IEEE Trans Microw Guided Wave Lett, 2000, 10: 400–402
33 Paknys R, Jackson D R. The relation between creeping waves, leaky waves and surface waves. IEEE Trans Anten Propag, 2005, 53: 898–907
34 Zhang M, Li L W, Tian Y F. An efficient approach for extracting poles of Green's functions in general multilayered media. IEEE Trans Anten Propag, 2008, 56: 269–273
35 Daoxiang W, Kai-Ning E Y, Jian B, et al. A direct method for extracting surface waves of Green's functions in a multilayered medium. In: IEEE Antennas and Propagation Society International Symposium, Hong Kong, 2008. 4395–4398
36 Lang S. Complex Analysis. 4th ed. New York: Spriger-Verlag, 1999
37 Anemogiannis E, Glytsis E. Multilayer waveguides: efficient numerical analysis of general structures. J Lightwave Tech, 1992, 10: 1344–1351
38 Rodriguez-Berral R, Mesa F, Medina F. Systematic and efficient root finder for computing the modal spectrum of planar layered waveguides: Original Articles. Int J RF Microw Comput Aid Eng, 2003, 14: 73–83
39 Song Z, Zhou H X, Hu J, et al. Accurate evaluation of Green's functions in a layered medium by SDP-FLAM. Sci China Ser F-Inf Sci, 2009, 52: 867–875
40 Yuan M, Sakar T K, Salazar-Palma M. A direct discrete complex image method from the closed-form Green's functions in multilayered media. IEEE Trans Microw Theory Tech, 2005, 53: 1025–1032
41 Yuan M, Sakar T K. Computation of the Sommerfeld integral tails using the matrix pencil method. IEEE Trans Anten Propag, 2006, 54: 1358–1362
42 Yuan M, Zhang Y, De A, et al. Two-dimensional discrete complex image method (DCIM) for closed-form Green's function of arbitrary 3D structures in general multilayered media. IEEE Trans Anten Propag, 2008, 56: 1350–1357
43 Pan S G, Wolff I. Scalarization of dyadic spectral Green's functions and network formalism for three-dimensional full-wave analysis of planar lines and antennas. IEEE Trans Microw Theory Tech, 1994, 42: 2118–2127
44 Chow Y L, Yang J J, Fang D G, et al. A closed-form spatial Green's function for the thick microstrip substrate. IEEE Trans Microw Theory Tech, 1991, 39: 588–592
45 Rogier H, Ginste D V. A fast procedure to accurately determine leaky modes in multilayered planar dielectric substrates. IEEE Trans Microw Theory Tech, 2008, 56: 1413–1422
46 Kincaid D, Cheney W. Numerical Analysis: Mathematics of Scientific Computing. Wadsworth Group, American Mathemetical Society, 2002
47 Mosig J R, Melcon A A. Green's functions in lossy layered media: integration along the imaginary axis and asymptotic behavior. IEEE Trans Anten Propag, 2003, 51: 3200–3208
48 Boix R R, Mesa F, Medina F. Application of total least squares to the derivation of closed-form Green's functions for planar layered media. IEEE Trans Microw Theory Tech, 2007, 55: 268–280
49 Mesa F, Boix R R, Medina F. Closed-form expressions of multilayered planar Green's functions that account for the continuous spectrum in the far field. IEEE Trans Microw Theory Tech, 2008, 56: 1601–1614
50 Shuley N V, Boix R R, Medina F, et al. On the fast approximation of Green's functions in MPIE formulations for planar layered media. IEEE Trans Microw Theory Tech, 2002, 50: 2185–2192

Appendix

According to the stipulation in (8), all the basic formulae used in [19] can be rewritten into fractional forms as follows:

$$Z_n^h = \frac{Z_n^{h,>}}{Z_n^{h,<}} = \frac{\omega\mu_0\mu_{r,n}}{k_{n,z}} \tag{A1}$$

$$Z_n^e = \frac{Z_n^{e,>}}{Z_n^{e,<}} = \frac{k_{n,z}}{\omega\varepsilon_0\varepsilon_{r,n}}, \tag{A2}$$

$$\Gamma_{n,m}^p = \frac{\Gamma_{n,m}^{p,>}}{\Gamma_{n,m}^{p,<}} = \frac{Z_n^{p,>}\cdot Z_m^{p,<} - Z_n^{p,<}\cdot Z_m^{p,>}}{Z_n^{p,>}\cdot Z_m^{p,<} + Z_n^{p,<}\cdot Z_m^{p,>}}, \tag{A3}$$

$$\overrightarrow{\Gamma}_n^p = \frac{\overrightarrow{\Gamma}_n^{p,>}}{\overrightarrow{\Gamma}_n^{p,<}} = \frac{\Gamma_{n+1,n}^{p,>}\cdot\overrightarrow{\Gamma}_{n+1}^{p,<} + \Gamma_{n+1,n}^{p,<}\cdot\overrightarrow{\Gamma}_{n+1}^{p,>}\cdot t_{n+1}^p}{\Gamma_{n+1,n}^{p,<}\cdot\overrightarrow{\Gamma}_{n+1}^{p,<} + \Gamma_{n+1,n}^{p,>}\cdot\overrightarrow{\Gamma}_{n+1}^{p,>}\cdot t_{n+1}^p}, \tag{A4}$$

$$\overleftarrow{\Gamma}_n^p = \frac{\overleftarrow{\Gamma}_n^{p,>}}{\overleftarrow{\Gamma}_n^{p,<}} = \frac{\Gamma_{n-1,n}^{p,>}\cdot\overleftarrow{\Gamma}_{n-1}^{p,<} + \Gamma_{n-1,n}^{p,<}\cdot\overleftarrow{\Gamma}_n^{p,>}\cdot t_{n-1}^p}{\Gamma_{n-1,n}^{p,<}\cdot\overleftarrow{\Gamma}_{n-1}^{p,<} + \Gamma_{n-1,n}^{p,>}\cdot\overleftarrow{\Gamma}_{n-1}^{p,>}\cdot t_{n-1}^p}, \tag{A5}$$

$$\frac{1}{D_n^p} \doteq \frac{M_n^{p,>}}{M_n^{p,<}} = \frac{\overleftarrow{\Gamma}_n^{p,<}\cdot\overrightarrow{\Gamma}_n^{p,<}}{\overleftarrow{\Gamma}_n^{p,<}\cdot\overrightarrow{\Gamma}_n^{p,<} - \overleftarrow{\Gamma}_n^{p,>}\cdot\overrightarrow{\Gamma}_n^{p,>}\cdot t_n^p}, \tag{A6}$$

$$\sum_{s=1}^{4} R_{n,s}^p \mathrm{e}^{-\mathrm{j}k_{z,n}\gamma_{n,s}} \doteq \frac{\Sigma_n^{p,>}}{\Sigma_n^{p,<}} = \frac{\left[\begin{array}{l}\overrightarrow{\Gamma}_n^{p,>}\cdot\overleftarrow{\Gamma}_n^{p,<}\cdot\mathrm{e}^{-\mathrm{j}k_{z,n}\gamma_{n,1}} + \overrightarrow{\Gamma}_n^{p,<}\cdot\overleftarrow{\Gamma}_n^{p,>}\cdot\mathrm{e}^{-\mathrm{j}k_{z,n}\gamma_{n,2}} \\ +\overrightarrow{\Gamma}_n^{p,>}\cdot\overleftarrow{\Gamma}_n^{p,>}\cdot\left(\mathrm{e}^{-\mathrm{j}k_{z,n}\gamma_{n,3}} + \mathrm{e}^{-\mathrm{j}k_{z,n}\gamma_{n,4}}\right)\end{array}\right]}{\overrightarrow{\Gamma}_n^{p,<}\cdot\overleftarrow{\Gamma}_n^{p,<}}, \tag{A7}$$

$$\sum_{s=1}^{4} (-1)^s R_{n,s}^p \mathrm{e}^{-\mathrm{j}k_{z,n}\gamma_{n,s}} \doteq \frac{\widehat{\Sigma}_n^{p,>}}{\widehat{\Sigma}_n^{p,<}} = \frac{\left[\begin{array}{l}-\overrightarrow{\Gamma}_n^{p,>}\cdot\overleftarrow{\Gamma}_n^{p,<}\cdot\mathrm{e}^{-\mathrm{j}k_{z,n}\gamma_{n,1}} + \overrightarrow{\Gamma}_n^{p,<}\cdot\overleftarrow{\Gamma}_n^{p,>}\cdot\mathrm{e}^{-\mathrm{j}k_{z,n}\gamma_{n,2}} \\ +\overrightarrow{\Gamma}_n^{p,>}\cdot\overleftarrow{\Gamma}_n^{p,>}\cdot\left(-\mathrm{e}^{-\mathrm{j}k_{z,n}\gamma_{n,3}} + \mathrm{e}^{-\mathrm{j}k_{z,n}\gamma_{n,4}}\right)\end{array}\right]}{\overrightarrow{\Gamma}_n^{p,<}\cdot\overleftarrow{\Gamma}_n^{p,<}}, \tag{A8}$$

$$T_{n,m}^{p,\pm} = \frac{T_{n,m}^{p,\pm,>}}{T_{n,m}^{p,\pm,<}} = \frac{S_{n,n\pm1}^{p,\pm,>}\cdot\prod\limits_{n<i<m\mathrm{or}m<i<n}\mathrm{e}^{-\mathrm{j}k_{z,i}d_i}\cdot S_{i,i\pm1}^{p,\pm,>}}{S_{n,n\pm1}^{p,\pm,<}\cdot\prod\limits_{n<i<m\mathrm{or}m<i<n} S_{i,i\pm1}^{p,\pm,<}}, \tag{A9}$$

$$S_{i,i\pm1}^{p,\pm} = \frac{S_{i,i\pm1}^{p,\pm,>}}{S_{i,i\pm1}^{p,\pm,<}} = \frac{\overrightarrow{\overleftarrow{\Gamma}}_{i\pm1}^{p,<}\cdot\left(\Gamma_{i\pm1,i}^{p,>} + \Gamma_{i\pm1,i}^{p,<}\right)}{\Gamma_{i\pm1,i}^{p,<}\cdot\overrightarrow{\overleftarrow{\Gamma}}_{i\pm1}^{p,<} + \Gamma_{i\pm1,i}^{p,>}\cdot\overrightarrow{\overleftarrow{\Gamma}}_{i\pm1}^{p,>}\cdot t_{i\pm1}^p}. \tag{A10}$$

In (A10), the relationship of $\Gamma_{i,j}^p = -\Gamma_{j,i}^p$ is considered.

Hence, for the case $m = n$, the TLGFs can be rewritten as

$$V_i^p = \frac{1}{2}\cdot\frac{Z_n^{p,>}}{Z_n^{p,<}}\cdot\left[\mathrm{e}^{-\mathrm{j}k_{z,n}|z-z'|} + \frac{M_n^{p,>}}{M_n^{p,<}}\cdot\frac{\Sigma_n^{p,>}}{\Sigma_n^{p,<}}\right], \tag{A11}$$

$$V_v^p = \frac{1}{2}\cdot\left[\pm\mathrm{e}^{-\mathrm{j}k_{z,n}|z-z'|} - \frac{M_n^{p,>}}{M_n^{p,<}}\cdot\frac{\widehat{\Sigma}_n^{p,>}}{\widehat{\Sigma}_n^{p,<}}\right], \tag{A12}$$

$$I_i^p = \frac{1}{2}\cdot\left[\pm\mathrm{e}^{-\mathrm{j}k_{z,n}|z-z'|} + \frac{M_n^{p,>}}{M_n^{p,<}}\cdot\frac{\widehat{\Sigma}_n^{p,>}}{\widehat{\Sigma}_n^{p,<}}\right], \tag{A13}$$

$$I_v^p = \frac{1}{2}\cdot\frac{Y_n^{p,>}}{Y_n^{p,<}}\cdot\left[\mathrm{e}^{-\mathrm{j}k_{z,n}|z-z'|} - \frac{M_n^{p,>}}{M_n^{p,<}}\cdot\frac{\Sigma_n^{p,>}}{\Sigma_n^{p,<}}\right]. \tag{A14}$$

For the case $n < m$, the TLGFs can be rewritten as

$$V_i^p = \frac{1}{2}\frac{Z_n^{p,>}}{Z_n^{p,<}}\cdot\frac{T_{n,m}^{p,+,>}}{T_{n,m}^{p,+,<}}\cdot\frac{M_n^{p,>}}{M_n^{p,<}}\cdot\frac{\left[\begin{array}{l}\left(\overleftarrow{\Gamma}_n^{p,<}\cdot\mathrm{e}^{-\mathrm{j}k_{z,n}(z_{n+1}-z')} + \overleftarrow{\Gamma}_n^{p,>}\cdot\mathrm{e}^{-\mathrm{j}k_{z,n}(-2z_n+z_{n+1}+z')}\right) \\ \cdot\left(\overrightarrow{\Gamma}_m^{p,<}\cdot\mathrm{e}^{-\mathrm{j}k_{z,m}(-z_m+z)} + \overrightarrow{\Gamma}_m^{p,>}\cdot\mathrm{e}^{-\mathrm{j}k_{z,m}(-z_m+2z_{m+1}-z)}\right)\end{array}\right]}{\overleftarrow{\Gamma}_n^{p,<}\cdot\overrightarrow{\Gamma}_m^{p,<}}, \tag{A15}$$

$$V_v^p = \frac{1}{2}\frac{Z_m^{p,>}\cdot Y_n^{p,>}}{Z_m^{p,<}\cdot Y_n^{p,<}}\cdot\frac{T_{m,n}^{p,-,>}}{T_{m,n}^{p,-,<}}\cdot\frac{M_m^{p,>}}{M_m^{p,<}}\cdot\frac{\left[\begin{array}{l}\left(\overleftarrow{\Gamma}_n^{p,<}\mathrm{e}^{-\mathrm{j}k_{z,n}(z_{n+1}-z')} - \overleftarrow{\Gamma}_n^{p,>}\cdot\mathrm{e}^{-\mathrm{j}k_{z,n}(-2z_n+z_{n+1}+z')}\right) \\ \cdot\left(\overrightarrow{\Gamma}_m^{p,<}\cdot\mathrm{e}^{-\mathrm{j}k_{z,m}(-z_m+z)} + \overrightarrow{\Gamma}_m^{p,>}\cdot\mathrm{e}^{-\mathrm{j}k_{z,m}(-z_m+2z_{m+1}-z)}\right)\end{array}\right]}{\overleftarrow{\Gamma}_n^{p,<}\cdot\overrightarrow{\Gamma}_m^{p,<}}, \tag{A16}$$

$$I_i^p = \frac{1}{2}\frac{Z_n^{p,>}\cdot Y_m^{p,>}}{Z_n^{p,<}\cdot Y_m^{p,<}}\cdot\frac{T_{n,m}^{p,+,>}}{T_{n,m}^{p,+,<}}\cdot\frac{M_n^{p,>}}{M_n^{p,<}}\cdot\frac{\left[\begin{array}{l}\left(\overleftarrow{\Gamma}_n^{p,<}\mathrm{e}^{-\mathrm{j}k_{z,n}(z_{n+1}-z')} + \overleftarrow{\Gamma}_n^{p,>}\cdot\mathrm{e}^{-\mathrm{j}k_{z,n}(-2z_n+z_{n+1}+z')}\right) \\ \cdot\left(\overrightarrow{\Gamma}_m^{p,<}\mathrm{e}^{-\mathrm{j}k_{z,m}(-z_m+z)} - \overrightarrow{\Gamma}_m^{p,>}\cdot\mathrm{e}^{-\mathrm{j}k_{z,m}(-z_m+2z_{m+1}-z)}\right)\end{array}\right]}{\overleftarrow{\Gamma}_n^{p,<}\cdot\overrightarrow{\Gamma}_m^{p,<}}, \tag{A17}$$

$$I_v^p = \frac{1}{2}\frac{Y_n^{p,>}}{Y_n^{p,<}} \cdot \frac{T_{m,n}^{p,-,>}}{T_{m,n}^{p,-,<}} \cdot \frac{M_m^{p,>}}{M_m^{p,<}} \cdot \frac{\left[\begin{array}{l}\left(\overleftarrow{\Gamma}_n^{p,<}\mathrm{e}^{-\mathrm{j}k_{z,n}(z_{n+1}-z')} - \overleftarrow{\Gamma}_n^{p,>} \cdot \mathrm{e}^{-\mathrm{j}k_{z,n}(-2z_n+z_{n+1}+z')}\right) \\ \cdot\left(\overrightarrow{\Gamma}_m^{p,<} \cdot \mathrm{e}^{-\mathrm{j}k_{z,m}(-z_m+z)} - \overrightarrow{\Gamma}_m^{p,>} \cdot \mathrm{e}^{-\mathrm{j}k_{z,m}(-z_m+2z_{m+1}-z)}\right)\end{array}\right]}{\overleftarrow{\Gamma}_n^{p,<} \cdot \overrightarrow{\Gamma}_m^{p,<}}. \tag{A18}$$

For the case $n < m$, the TLGFs can be rewritten as

$$V_i^p = \frac{1}{2}\frac{Z_n^{p,>}}{Z_n^{p,<}} \cdot \frac{T_{n,m}^{p,-,>}}{T_{n,m}^{p,-,<}} \cdot \frac{M_n^{p,>}}{M_n^{p,<}} \cdot \frac{\left[\begin{array}{l}\left(\overrightarrow{\Gamma}_n^{p,<} \cdot \mathrm{e}^{-\mathrm{j}k_{z,n}(-z_n+z')} + \overrightarrow{\Gamma}_n^{p,>} \cdot \mathrm{e}^{-\mathrm{j}k_{z,n}(2z_{n+1}-z_n-z')}\right) \\ \cdot\left(\overleftarrow{\Gamma}_m^{p,<} \cdot \mathrm{e}^{-\mathrm{j}k_{z,m}(z_{m+1}-z)} + \overleftarrow{\Gamma}_m^{p,>} \cdot \mathrm{e}^{-\mathrm{j}k_{z,m}(-2z_m+z_{m+1}+z)}\right)\end{array}\right]}{\overrightarrow{\Gamma}_n^{p,<} \cdot \overleftarrow{\Gamma}_m^{p,<}}, \tag{A19}$$

$$V_v^p = \frac{1}{2}\frac{Z_m^{p,>} \cdot Y_n^{p,>}}{Z_m^{p,<} \cdot Y_n^{p,<}} \cdot \frac{T_{m,n}^{p,+,>}}{T_{m,n}^{p,+,<}} \cdot \frac{M_m^{p,>}}{M_m^{p,<}} \cdot \frac{\left[\begin{array}{l}\left(-\overrightarrow{\Gamma}_n^{p,<} \cdot \mathrm{e}^{-\mathrm{j}k_{z,n}(-z_n+z')} + \overrightarrow{\Gamma}_n^{p,>} \cdot \mathrm{e}^{-\mathrm{j}k_{z,n}(2z_{n+1}-z_n-z')}\right) \\ \cdot\left(\overleftarrow{\Gamma}_m^{p,<} \cdot \mathrm{e}^{-\mathrm{j}k_{z,m}(z_{m+1}-z)} + \overleftarrow{\Gamma}_m^{p,>} \cdot \mathrm{e}^{-\mathrm{j}k_{z,m}(-2z_m+z_{m+1}+z)}\right)\end{array}\right]}{\overrightarrow{\Gamma}_n^{p,<} \cdot \overleftarrow{\Gamma}_m^{p,<}}, \tag{A20}$$

$$I_i^p = \frac{1}{2}\frac{Z_n^{p,>} \cdot Y_m^{p,>}}{Z_n^{p,<} \cdot Y_m^{p,<}} \cdot \frac{T_{n,m}^{p,-,>}}{T_{n,m}^{p,-,<}} \cdot \frac{M_n^{p,>}}{M_n^{p,<}} \cdot \frac{\left[\begin{array}{l}\left(\overrightarrow{\Gamma}_n^{p,<} \cdot \mathrm{e}^{-\mathrm{j}k_{z,n}(-z_n+z')} + \overrightarrow{\Gamma}_n^{p,>} \cdot \mathrm{e}^{-\mathrm{j}k_{z,n}(2z_{n+1}-z_n-z')}\right) \\ \cdot\left(-\overleftarrow{\Gamma}_m^{p,<} \cdot \mathrm{e}^{-\mathrm{j}k_{z,m}(z_{m+1}-z)} + \overleftarrow{\Gamma}_m^{p,>} \cdot \mathrm{e}^{-\mathrm{j}k_{z,m}(-2z_m+z_{m+1}+z)}\right)\end{array}\right]}{\overrightarrow{\Gamma}_n^{p,<} \cdot \overleftarrow{\Gamma}_m^{p,<}}, \tag{A21}$$

$$I_v^p = \frac{1}{2}\frac{Y_n^{p,>}}{Y_n^{p,<}} \cdot \frac{T_{m,n}^{p,+,>}}{T_{m,n}^{p,+,<}} \cdot \frac{M_m^{p,>}}{M_m^{p,<}} \cdot \frac{\left[\begin{array}{l}\left(-\overrightarrow{\Gamma}_n^{p,<} \cdot \mathrm{e}^{-\mathrm{j}k_{z,n}(-z_n+z')} + \overrightarrow{\Gamma}_n^{p,>} \cdot \mathrm{e}^{-\mathrm{j}k_{z,n}(2z_{n+1}-z_n-z')}\right) \\ \cdot\left(-\overleftarrow{\Gamma}_m^{p,>} \cdot \mathrm{e}^{-\mathrm{j}k_{z,m}(z_{m+1}-z)} + \overleftarrow{\Gamma}_m^{p,<} \cdot \mathrm{e}^{-\mathrm{j}k_{z,m}(-2z_m+z_{m+1}+z)}\right)\end{array}\right]}{\overrightarrow{\Gamma}_n^{p,<} \cdot \overleftarrow{\Gamma}_m^{p,>}}. \tag{A22}$$

For analytically calculating residues of all SWPs, the derivatives of the generalized reflection coefficients are also necessary, which are given as follows:

$$\begin{cases}(Z_n^{h,>})' = 0, \\ (Z_n^{h,<})' = -k_\rho/k_{n,z},\end{cases} \tag{A23}$$

$$\begin{cases}(Z_n^{e,>})' = -k_\rho/k_{n,z}, \\ (Z_n^{e,<})' = 0.\end{cases} \tag{A24}$$

$$(t_n^p)' = \mathrm{e}^{-\mathrm{j}2k_{z,n}d_n} \cdot \frac{j2d_n \cdot k_\rho}{k_{z,n}}, \tag{A25}$$

$$(\Gamma_{n,m}^{p,>})' = [(Z_n^{p,>})' \cdot Z_m^{p,<} + Z_n^{p,>} \cdot (Z_m^{p,<})'] - [(Z_n^{p,<})' \cdot Z_m^{p,>} + Z_n^{p,<} \cdot (Z_m^{p,>})'], \tag{A26}$$

$$(\Gamma_{n,m}^{p,<})' = [(Z_n^{p,>})' \cdot Z_m^{p,<} + Z_n^{p,>} \cdot (Z_m^{p,<})'] + [(Z_n^{p,<})' \cdot Z_m^{p,>} + Z_n^{p,<} \cdot (Z_m^{p,>})'], \tag{A27}$$

$$\begin{aligned}(\overrightarrow{\Gamma}_n^{p,>})' = {} & (\Gamma_{n+1,n}^{p,>})' \cdot \overrightarrow{\Gamma}_{n+1}^{p,<} + \Gamma_{n+1,n}^{p,>} \cdot (\overrightarrow{\Gamma}_{n+1}^{p,<})' + (\Gamma_{n+1,n}^{p,<})' \cdot \overrightarrow{\Gamma}_{n+1}^{p,>} \cdot t_{n+1}^p + \Gamma_{n+1,n}^{p,<} \cdot (\overrightarrow{\Gamma}_{n+1}^{p,>})' \cdot t_{n+1}^p \\ & + \Gamma_{n+1,n}^{p,<} \cdot \overrightarrow{\Gamma}_{n+1}^{p,>} \cdot (t_{n+1}^p)',\end{aligned} \tag{A28}$$

$$\begin{aligned}(\overrightarrow{\Gamma}_n^{p,<})' = {} & (\Gamma_{n+1,n}^{p,<})' \cdot \overrightarrow{\Gamma}_{n+1}^{p,<} + \Gamma_{n+1,n}^{p,<} \cdot (\overrightarrow{\Gamma}_{n+1}^{p,<})' + (\Gamma_{n+1,n}^{p,>})' \cdot \overrightarrow{\Gamma}_{n+1}^{p,>} \cdot t_{n+1}^p + \Gamma_{n+1,n}^{p,>} \cdot (\overrightarrow{\Gamma}_{n+1}^{p,>})' \cdot t_{n+1}^p \\ & + \Gamma_{n+1,n}^{p,>} \cdot \overrightarrow{\Gamma}_{n+1}^{p,>} \cdot (t_{n+1}^p)',\end{aligned} \tag{A29}$$

$$\begin{aligned}(\overleftarrow{\Gamma}_n^{p,>})' = {} & (\Gamma_{n-1,n}^{p,>})' \cdot \overleftarrow{\Gamma}_{n-1}^{p,<} + \Gamma_{n-1,n}^{p,>} \cdot (\overleftarrow{\Gamma}_{n-1}^{p,<})' + (\Gamma_{n-1,n}^{p,<})' \cdot \overleftarrow{\Gamma}_{n-1}^{p,>} \cdot t_{n-1}^p + \Gamma_{n-1,n}^{p,<} \cdot (\overleftarrow{\Gamma}_{n-1}^{p,>})' \cdot t_{n-1}^p \\ & + \Gamma_{n-1,n}^{p,<} \cdot \overleftarrow{\Gamma}_{n-1}^{p,>} \cdot (t_{n-1}^p)',\end{aligned} \tag{A30}$$

$$\begin{aligned}(\overleftarrow{\Gamma}_n^{p,<})' = {} & (\Gamma_{n-1,n}^{p,<})' \cdot \overleftarrow{\Gamma}_{n-1}^{p,<} + \Gamma_{n-1,n}^{p,<} \cdot (\overleftarrow{\Gamma}_{n-1}^{p,<})' + (\Gamma_{n-1,n}^{p,>})' \cdot \overleftarrow{\Gamma}_{n-1}^{p,>} \cdot t_{n-1}^p + \Gamma_{n-1,n}^{p,>} \cdot (\overleftarrow{\Gamma}_{n-1}^{p,>})' \cdot t_{n-1}^p \\ & + \Gamma_{n-1,n}^{p,>} \cdot \overleftarrow{\Gamma}_{n-1}^{p,>} \cdot (t_{n-1}^p)',\end{aligned} \tag{A31}$$

$$\begin{aligned}(S_{i,i\pm1}^{p,\pm,<})' = {} & (\Gamma_{i\pm1,i}^{p,<})' \cdot \overrightarrow{\overrightarrow{\Gamma}}_{i\pm1}^{p,<} + \Gamma_{i\pm1,i}^{p,<} \cdot (\overrightarrow{\overrightarrow{\Gamma}}_{i\pm1}^{p,<})' + (\Gamma_{i\pm1,i}^{p,>})' \cdot \overrightarrow{\overrightarrow{\Gamma}}_{i\pm1}^{p,>} \cdot \mathrm{e}^{-\mathrm{j}k_{z,i\pm1}d_{i\pm1}} \\ & + \Gamma_{i\pm1,i}^{p,>} \cdot (\overrightarrow{\overrightarrow{\Gamma}}_{i\pm1}^{p,>})' \cdot \mathrm{e}^{-\mathrm{j}k_{z,i\pm1}d_{i\pm1}} + \Gamma_{i\pm1,i}^{p,>} \cdot \overrightarrow{\overrightarrow{\Gamma}}_{i\pm1}^{p,>} \cdot (t_{i\pm1}^p)',\end{aligned} \tag{A32}$$

$$(T_{n,m}^{p,\pm,<})' = (S_{n,n\pm1}^{p,\pm,<})' \cdot \prod_{\substack{n<i<m \\ \mathrm{or}\, m<i<n}} S_{i,i\pm1}^{p,\pm,<} + S_{n,n\pm1}^{p,\pm,<} \cdot \sum_{\substack{n<s<m \\ \mathrm{or}\, m<s<n}} \left[(S_{s,s\pm1}^{p,\pm,<})' \cdot \prod_{\substack{n<i<m \\ \mathrm{or}\, m<i<n \\ i\neq s}} S_{i,i\pm1}^{p,\pm,<}\right]. \tag{A33}$$